ACS chemical biology

Articles

Cite This: ACS Chem. Biol. 2018, 13, 600−608

Rational-Differential Design of Highly Specific Glycomimetic Ligands: Targeting DC-SIGN and Excluding Langerin Recognition

Vanessa Porkolab,[†] Eric Chabrol,[†] Norbert Varga,[‡] Stefania Ordanini,[‡] Ieva Sutkevičiūtė,[†] Michel Thépaut,[†] Maria José García-Jiménez,[§] Eric Girard,[†] Pedro M. Nieto,[§] Anna Bernardi,*[,‡] and Franck Fieschi*[,†]

[†]Univ. Grenoble Alpes, CNRS, CEA, Institut de Biologie Structurale, F-38044 Grenoble, France

[‡]Università degli Studi di Milano (UniMI), Dip. Chimica, via Golgi 19, 20133, Milano, Italy

[§]Glycosystems Laboratory, Instituto de Investigaciones Químicas (IIQ), Centro de Investigaciones Científicas Isla de La Cartuja, CSIC and Universidad de Sevilla, Américo Vespucio, 49, 41092 Sevilla, Spain

Supporting Information

ABSTRACT: At the surface of dendritic cells, C-type lectin receptors (CLRs) allow the recognition of carbohydrate-based PAMPS or DAMPS (pathogen- or danger-associated molecular patterns, respectively) and promote immune response regulation. However, some CLRs are hijacked by viral and bacterial pathogens. Thus, the design of ligands able to target specifically one CLR, to either modulate an immune response or to inhibit a given infection mechanism, has great potential value in therapeutic design. A case study is the selective blocking of DC-SIGN, involved notably in HIV trans-infection of T lymphocytes, without interfering with langerin-mediated HIV clearance. This is a challenging task due to their overlapping carbohydrate specificity. Toward the rational design of DC-SIGN selective ligands, we performed a comparative affinity study between DC-SIGN and langerin with natural ligands. We found that GlcNAc is recognized by both CLRs; however, selective sulfation are shown to increase the selectivity in favor of langerin. With the combination of site-directed mutagenesis and X-ray structural analysis of the langerin/GlcNS6S complex, we highlighted that 6-sulfation of the carbohydrate ligand induced langerin specificity. Additionally, the K313 residue from langerin was identified as a critical feature of its binding site. Using a rational and a differential approach in the study of CLR binding sites, we designed, synthesized, and characterized a new glycomimetic, which is highly specific for DC-SIGN vs langerin. STD NMR, SPR, and ITC characterizations show that compound 7 conserved the overall binding mode of the natural disaccharide while possessing an improved affinity and a strict specificity for DC-SIGN

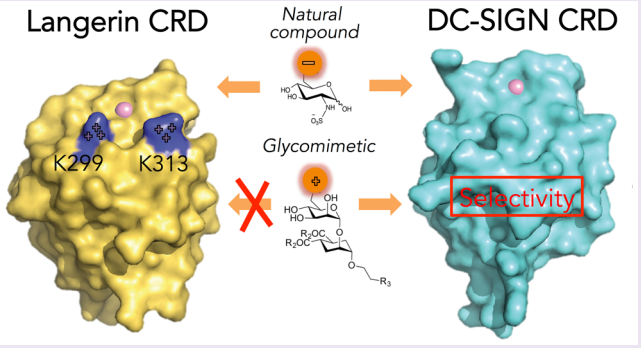

C-type lectin receptors (CLRs) are central sensing systems for the regulation of the initial immune response through dendritic cells.[1,2] Together with the toll-like receptor (TLR) family of pathogen recognition receptors (PRRs), they are key elements in the recognition of both pathogen-associated molecular patterns (PAMPs) and danger-associated molecular patterns (DAMPs) displayed by altered cells. Dendritic cells use CLRs to recognize carbohydrate-based PAMPs or DAMPs in a Ca^{2+}-dependent manner. Upon recognition, and depending on the crosstalk with TLRs, an activation or tolerance response will be promoted by dendritic cells toward specific T-cells.[3,4] Apart from being essentials for immune regulation, some of these CLRs are also hijacked by pathogens during their infection process. For instance, LSECtin and DC-SIGN are used to this purpose respectively by the Ebola virus and by a wide range of virus and bacterial pathogens (from HIV, *M. tuberculosis*, to *C. albicans* for DC-SIGN).[5−9] Thus, CLRs have become attractive targets for the design of new ligands able to modulate the immune response toward activation or inhibition as a function of the CLRs addressed. Such ligands could become anti-infective agents in cases where CLRs are used by pathogens to infect the host.

The development of such ligands as molecular probes for the modulation of various CLRs is the subject of intense efforts.[10−12] However, the development of highly specific and effective ligands toward CLRs faces several specific bottlenecks. The first problem is the nature of the natural ligands, oligosaccharides, that are easily metabolized and that may have a low level of bioavailability under therapeutic conditions. Second, natural carbohydrates frequently bind within CLRs' Ca^{2+} binding sites using multiple binding modes, thus making the specific benefit of any targeted modification almost

Received: November 6, 2017
Accepted: December 22, 2017
Published: December 22, 2017

DOI: 10.1021/acschembio.7b00958
ACS Chem. Biol. 2018, 13, 600−608

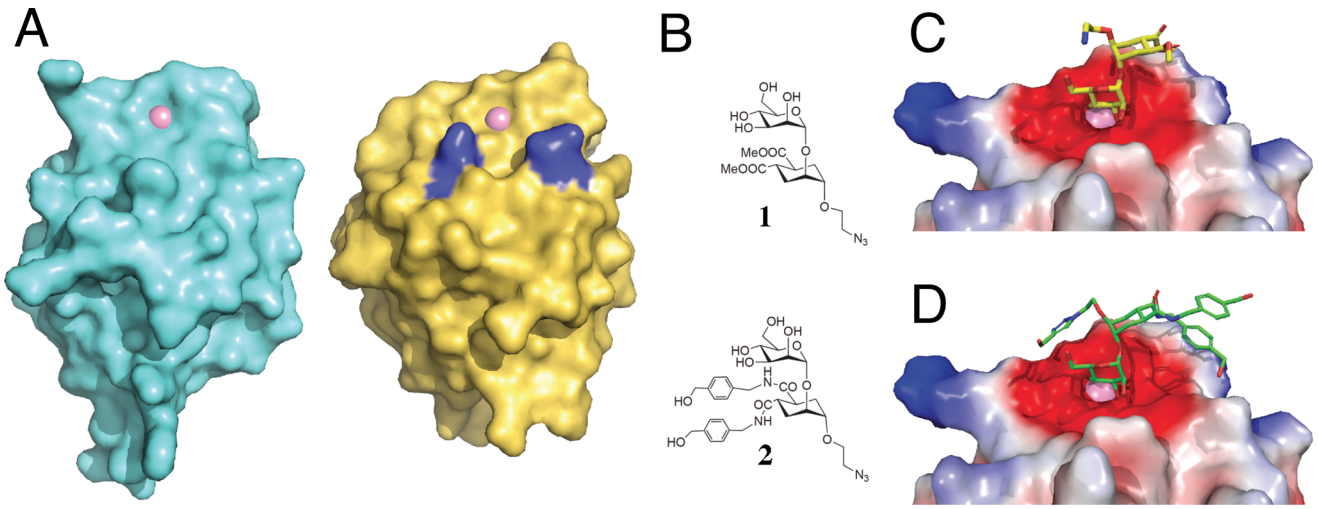

Figure 1. Structural comparison and glycomimetic design targeting the carbohydrate binding domain of DC-SIGN vs langerin. (A) Surface representation of DC-SIGN CRD (cyan, PDB 2it6) and langerin CRD (yellow, PDB 3c22). Ca^{2+} ions within the binding site are in pink. The two langerin specific lysines, K299 and K313, are represented in dark blue. (B) Structure of two generations of glycomimetic directed against DC-SIGN. (C and D). Electrostatic surfaces of DC-SIGN CRD in complex with **1** (PDB 2xr5) and **2** (STD NMR and molecular docking).

unpredictable. Indeed, depending on the mode of binding, a given structural modification of a ligand may either improve or reduce and even eliminate the binding affinity. Third, the active sites of CLRs are shallow binding pockets and open to the solvent (Figure 1A), contributing to low affinity ligands, often in the millimolar range. And finally, designed ligands often generate off-target effects due to carbohydrate cross-recognition between various CLRs. Altogether, these barriers make the rational design of tightly bound and CLR-selective ligands difficult. Despite these challenges, methods in carbohydrate chemistry and structure-based design have progressed, opening the door to successes in CLR ligand design.

DC-SIGN, one of the most investigated CLRs up to now, is a good example of the cumulative difficulties typically encountered with CLRs. To date, issues involving biostability and bioavailability,[13−16] heterogeneous modes of binding with the Ca^{2+} binding site, and weak protein−carbohydrate affinity have been successfully addressed for DC-SIGN by several groups.[13,17−19] Our previous work set out to rationally design glycosidase-resistant glycomimetic ligands that bound to DC-SIGN with binding modes similar to the natural ligands. From this approach, we identified two glycomimetics, a pseudodi- and a pseudotrisaccharide, as lead compounds able to bind efficiently DC-SIGN and even to be effective in anti-HIV *trans*-infection test (Figure 1B).[20−22] However, because of the unpredictable multiple binding mode of carbohydrates with CLRs,[23−25] we have been able to establish that only the pseudodisaccharide **1** meets the requirement of a unique binding mode within DC-SIGN (Figure 1C) and allows further rational molecule improvement.

Using structural information regarding the binding mode of this glycomimetic,[23] we rationally improved the relative affinity of compound **1** for DC-SIGN by substituting the methyl ester groups on the cyclohexane moiety with the amides in compound **2**. The extended ligand surface contact within the binding site leads to an improvement of its affinity.[26] Other groups, also using structural information and molecular modeling, have been successful in affinity improvement of monovalent ligands.[15,27,28] However, further affinity improvements in the low micromolar or even the nanomolar ranges have been reached only using multivalent presentations of lead ligands on molecular scaffolds.[18,29−32] On the other hand, the carbohydrate cross-recognition between different CLRs has not been addressed specifically up to now. During the development of compound **2**, we discovered a fortuitous selectivity increase in favor of DC-SIGN relative to langerin, another CLR also able to recognize HIV envelope glycoprotein, gp120.[23,26] However, even if some selectivity could be obtained, the remaining activity toward langerin is not negligible, particularly in a multivalent presentation that will also improve this nondesired interaction. The case study of DC-SIGN and langerin is of particular interest due to their opposite physiological consequences, respectively as promoting the T-lymphocytes infection or contributing to virus elimination.[7,33−35] In addition, langerin targets HIV to Birbeck granules, which are believed to be an atypical antigen processing pathway to Langerhans cells.[33,36] For all of these reasons, the design of specific and selective antagonists for DC-SIGN over langerin is fully justified.

Here, in this work, we address specifically the unsolved problem of CLR cross-recognition. We pioneer a differential rational design approach by which we analyze the structural and functional variances between the two binding sites, developing ligands that favor DC-SIGN and disfavor recognition by langerin. Differential rational design aims to reach a complete specificity for DC-SIGN. Here, the DC-SIGN/langerin pair is used as a case study for potential applications in the design of HIV capture inhibitors and of immune regulation therapeutics.

RESULTS

Sulfation-Induced Selectivity toward Langerin. The main difference in ligand recognition between DC-SIGN and langerin lies in the ability of langerin to specifically recognize sulfated glycans. In order to design ligand modifications to generate specific glycomimetic candidates, recognition of sulfated glycans by langerin needs to be understood. Langerin recognizes sulfated glycans with terminal 6-SO_4−Gal residues[37,38] or glycosaminoglycans containing sulfated derivatives of *N*-acetyl-D-glucosamine (GlcNAc).[39,40] Because GlcNAc and Man share the same 3,4-diequatorial hydroxyl groups for

DOI: 10.1021/acschembio.7b00958
ACS Chem. Biol. 2018, 13, 600−608

binding to Ca^{2+}, the binding mode of GlcNAc derivatives is expected to be similar to that of Man. Thus, we focused our selectivity characterization on GlcNAc-sulfated derivatives in order to compare and transfer newly identified features to the mannose-based glycomimetic lead compound **1**.

The different sulfated versions of *N*-acetyl-D-glucosamine evaluated for their relative affinity (IC_{50}) for DC-SIGN and langerin are presented in Figure 2A, B, and C. Nonsulfated

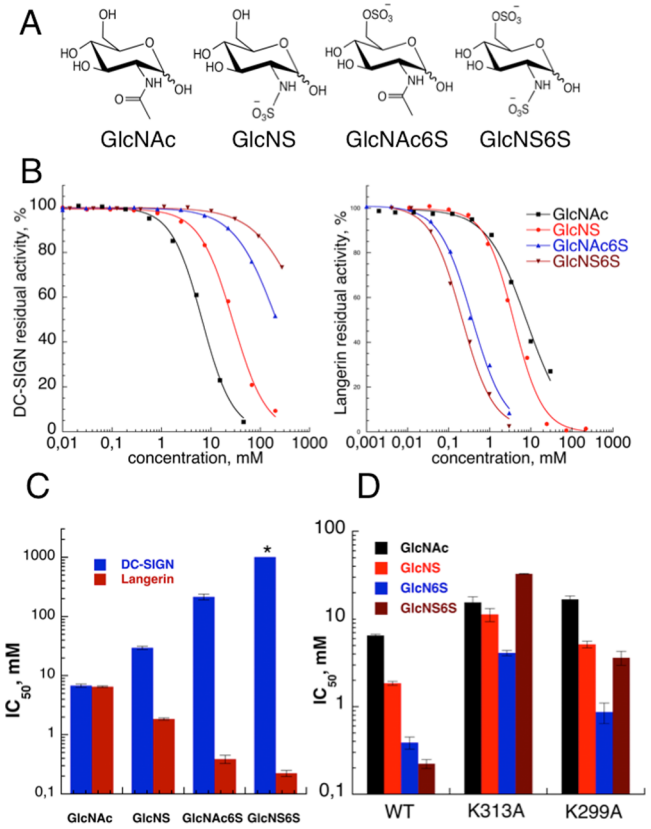

Figure 2. Inhibition of DC-SIGN and langerin binding to Man-BSA by sulfated derivatives of GlcNAc in a SPR competition assay. (A) Structure of GlcNAc-sulfated derivatives used in the study. (B) Inhibition curves for DC-SIGN (left) and langerin (right). (C) Comparison of IC_{50}, extracted from B, for DC-SIGN (blue) or langerin (red), as a function of the sulfation degree and position. (D) Impact of lysine mutations in langerin on the IC_{50} of GlcNAc sulfated-derivatives. IC_{50}, extracted from SPR derived inhibitions curves, is presented as a function of the GlcNAc sulfation pattern and for a given version of langerin (see SI Material and Methods for corresponding sensorgrams and inhibitory curves). (*) For GlcNS6S, the IC_{50} for DC-SIGN has not been reached experimentally (see from B) and thus extrapolated from the inhibition curve equation.

GlcNAc has the same affinity for both lectins (5 mM, Figure 2C and Table S2 in the Supporting Information) and comparable with the reported affinity of mannose for DC-SIGN.[21] However, adding one or several negative sulfate groups onto the ligand results in an increase in affinity in favor of langerin, while recognition by DC-SIGN drastically decreases. This results in a selectivity factor of 5000 in favor of langerin as measured for the disulfated ligand, GlcNS6S. Significantly, a single sulfation at position 6 of GlcNAc is responsible for a selectivity factor close to 600 (IC_{50} of 0.39 mM and 0.22 mM for GlcNAc6S and GlcNS6S, respectively).

Recognition Mechanism of Sulfated Ligands. The interaction of sulfated saccharides is a unique feature of langerin compared to DC-SIGN. To understand determinants of this specificity, we analyzed the affinities of sulfated ligands with two active site mutants of the langerin-extracellular domain (Lg-ECD). We studied the roles of lysines 299 and 313 (Figure 1A), which are ideally positioned in the Ca^{2+} site surroundings. Figure 2D summarizes the IC_{50}, determined by SPR inhibition assay, for each ligand as a function of the Lg-ECD mutations. Lysine mutations induce an overall decrease in affinity of the sulfated ligand for langerin (Figure 2D and Table S2). Mutation K313A completely abolishes the improved affinity observed upon sulfation of the ligands. In addition, the K299A mutation leads to a 2-fold reduction in GlcNAc6S ligand IC_{50} when compared to wild type langerin. This effect is more pronounced for the K313A mutant, with a decrease of the affinity of GlcNAc6S for langerin by a factor of 10. The key role of lysine 313 is also observed in the crystallographic structure of the Lg-carbohydrate recognition domain (CRD) with GlcNS6S.

X-ray Crystal Structure of Lg-CRD/GlcNS6S Complex. The crystal contains four copies of the CRD per asymmetric unit within a $P4_2$ space group. The structure solved at 1.89 Å is well conserved when compared to previously determined structures of Lg-CRD as illustrated by RMSDs of 0.443, 0.335, and 0.331 Å with Lg-CRD structures without a ligand or complexed with $6SO_4$−Galß1−4GlcNAC or Manα1−2Man (PDB codes are 3c22, 3p5i, and 3p5f, respectively).[38,41] As structure resolution was conducted by molecular replacement using an unliganded Lg-CRD model, the identification of a well-defined electron density onto the Ca^{2+} ion allowed clear establishment of the presence of the GlcNS6S ligand within the binding site (Figure 3A). As expected, GlcNS6S binds to the Ca^{2+} ion with its equatorial 3-OH and 4-OH groups. The anomeric OH group interacts with K299. Pertaining to the sulfate groups, the 6-sulfate is involved in an electrostatic interaction with K313, and the N-sulfate in C_2 is oriented toward the solvent (Figure 3B). In addition, three water molecules connect the ligand to the protein (see Supporting Information, Figure S1).

It appears that K299 has a minor role in the binding whereas the K313 plays a preponderant role in the affinity of 6-sulfated ligands (Figure 3C), in agreement with the impact of K313A mutation reported above. However, both lysines contribute to the establishment of a strong positive electrostatic region, adjacent to the Ca^{2+} binding site, that allows to accommodate diverse sulfated glycans (Figure 3C). For instance, in the binding mode of $6SO_4$−Galß1−4GlcNac, the sulfate group of Gal6S was clearly oriented between K313 and K299. In that case, the two lysines were both essential to the sulfate recognition.[38,42,43] Recently, we characterized the binding mode to Lg-CRD of eight heparin-derived trisaccharides, composed of GlcN−IdoA−GlcN, with different sulfation patterns.[40] In all cases, it is the terminal nonreducing GlcN that is binding to the Ca^{2+} ion. The IdoA and GlcN residues extend between K313 and K299 and establish secondary contacts with the langerin surface. Here, it emerges that these two lysines are dynamic in their interactions with the sulfate group. Notably, K313 can shift to accommodate various sulfated ligands (see SI Figure S2).

Aiming to develop a highly specific antagonist of DC-SIGN versus langerin, the observation that a negative charge on the sugar C_6 specifically interacts with K313 of the langerin binding site represents the starting point for a glycomimetic design

DOI: 10.1021/acschembio.7b00958
ACS Chem. Biol. 2018, 13, 600−608

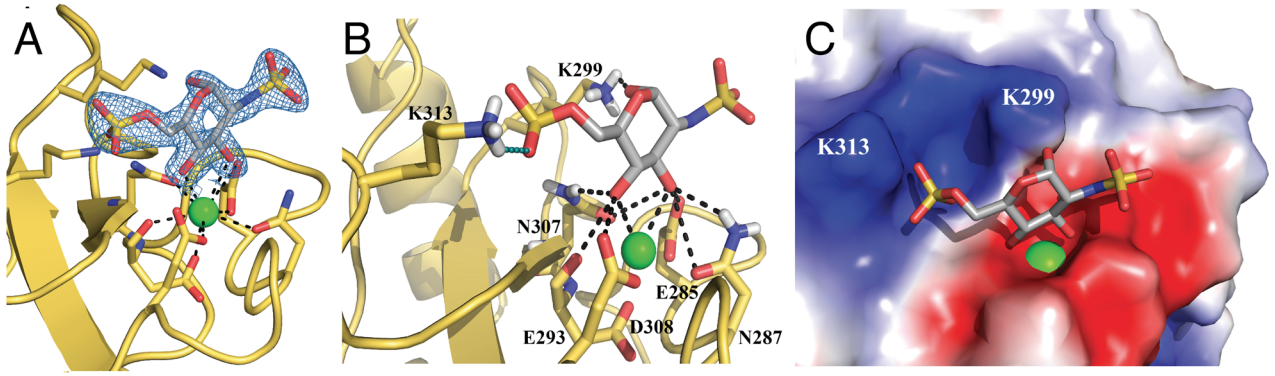

Figure 3. Binding mode of GlcNS6S within langerin calcium binding site. (A) Electron density map for bound GlcNS6S. The bound ligand is shown superimposed on the F_o-F_c electron density map contoured at 3σ. Bonds involved in Ca^{2+} binding are in black dashed line. (B) Interaction network involved in GlcNS6S interaction. Black dashed line for polar interaction and green dashed line for ionic bond. (C) Electrostatic potential of Lg-CRD surface in the Lg-CRD/GlcNS6S complex highlights the positive area around K313 and K299 positions.

strategy. The X-ray structure of the DC-SIGN complex with glycomimetic **1**[23] shows that the C_6 position of the sugar unit is not involved in any direct interaction (Figure 1C), and it is located in a very open area, close to a negatively charged patch of the DC-SIGN surface. A positive charge and/or a steric hindrance in position C_6 of **1** should lead to an electrostatic repulsion or steric clashes with K313 within the langerin binding site. Glycomimetics modified in position C_6 are expected to differentially impact binding to langerin and to DC-SIGN.

DC-SIGN vs Langerin Selectivity of Pseudodisaccharide Mimetics: Design of Third-Generation Ligand 7. On the basis of the lead compound **1**, we synthesized a novel group of four compounds modified at position 6 of the mannose ring (compounds **3**–**6**, Figure 4, see Supporting Information for

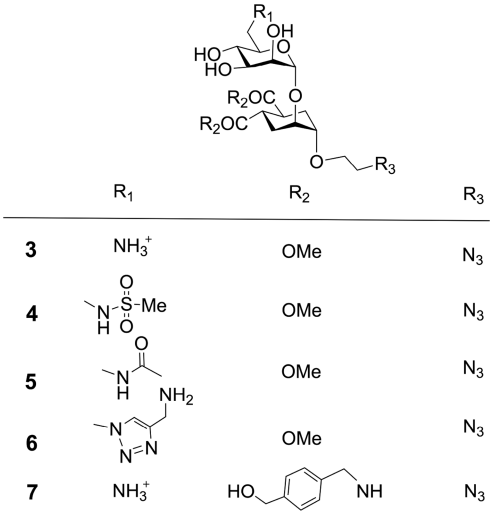

Figure 4. Structure of 6-modified pseudodimannosides **3**–**7**.

experimental details) and analyzed their DC-SIGN vs langerin selectivity using SPR. SPR competition studies with compound **1** or its 6-amino counterpart, compound **3** (Table 1), clearly showed a strong enhancement of DC-SIGN selectivity in compound **3**.

While the selectivity is a modest 1.54 for the initial lead **1**, compound **3** reaches a selectivity factor above 7. We also observed that the relative affinity for DC-SIGN was improved (IC_{50} = 481 μM), compared to the lead compound **1** (IC_{50} = 956 μM). Thus, as expected, the positively charged amino group results in an improvement of DC-SIGN affinity and selectivity.

The effect of the 6-amino group in DC-SIGN binding was analyzed using NMR transient methods (STD-NMR and NOESY experiments for the complex and the free mimic).[44] STD NMR consists of a selective irradiation of the receptor in the presence of a ligand. If the ligand is bound to the receptor, it will receive some magnetization transferred from the protein in an amount that is dependent on the proximity of the contact.[44] Transfer NOE, performed in the presence of a small amount of the receptor, relies on the larger correlation time acquired by the ligand when it is forming part of the macromolecular complex; this causes larger and faster NOE effects that are averaged across the signals of the free ligand when the association–dissociation equilibrium is fast enough.[44] The triazole modified analogs **1-T** and **3-T** (Figure 5) allow a better dispersion of NMR signals but do not modify the binding process and the geometry of the bound conformation.[26] Indeed, this analysis strongly suggested that **1-T** and **3-T** share a common binding mode with DC-SIGN (see Supporting Information data). As discussed in the introduction, compound **2** had been previously selected as a first optimization of **1**, on the basis of its relative DC-SIGN affinity (3 times improvement of the IC_{50}).[26] Its binding mode to DC-SIGN, characterized by STD NMR (Figure 1D),[26] is also conserved, and the additional hydroxymethylene-benzyl groups increase the surface contact of the ligand within the DC-SIGN binding site. The langerin screening reported in Table 1 shows an unexpected selectivity improvement of **2** over **1** by a factor of 7. Thus, the third-generation mimic **7**, combining the two modifications of second-generation **2** and **3** (Figure 4), was synthesized.

A quantitative STD-NMR analysis of **7-T** was frustrated by spectral congestion. Attempts to solve the signal overlap by including a second $^1H-^{13}C$ transference after the STD module using an HSQC to spread the peaks along a second dimension were unsuccessful due to low signal. Thus, for the study of the DC-SIGN interaction of **7-T**, we rely only on the transfer NOE data, obtained in the presence of DC-SIGN, reflecting the structural properties of the bound conformation. Transfer NOESY experiments clearly showed the exclusive NOE of the extended conformation as for **3-T** (Figure 5 and Figure S12, for full spectrum, in Supporting Information); consequently, we can assess that bound conformations of **3-T** and **7-T** are equivalent.

DOI: 10.1021/acschembio.7b00958
ACS Chem. Biol. 2018, 13, 600–608

Table 1. Evaluation of Glycomimetics Inhibition Potency Towards DC-SIGN and langerin (SPR)[a]

	IC50 (μM)			Inhibition (%) at 4.4 mM	
compounds	DC-SIGN	langerin	selectivity	DC-SIGN	langerin
Manα1−2Man	915 ± 25	1680 ± 61	1.83	89.8	74.6
1	956 ± 38	1474 ± 329	1.54	83.3	40.8
2	329 ± 5	2556 ± 610	7.76	99.6	36.3
3	481 ± 11	3440 ± 668	7.15	97.3	41.9
4	703 ± 29	1236 ± 215	1.75	n.d.	n.d.
5	1235 ± 40	1933 ± 90	1.56	n.d.	n.d.
6	1366 ± 81	4035 ± 145	2.95	n.d.	n.d.
7	254 ± 5	>4400	n.a.	99.7	0

[a]n.a., not applicable; n.d., not determined.

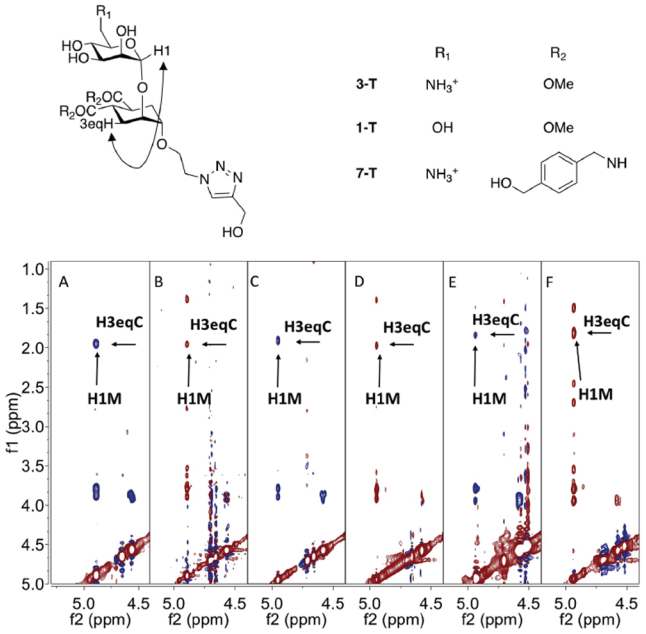

Figure 5. Triazole derivatives **1-T**, **3-T**, and **7-T** formulas showing the NOE between H1 from mannose and H3 equatorial of cyclohexyl moiety characteristic of an extended geometry (top). Expansions of NOESY (A, C, E) and transfer NOESY (B, D, F) experiments for **3-T** (A and B), **1-T** (C and D), and **7-T** (E and F). Cross-peaks corresponding with the NOE between mannose anomeric proton H1M and H3 equatorial of cyclohexyl are labeled (bottom). Peaks belonging to the central cyclohexyl moiety of **7-T** are negative contrasting with **3-T** and **1-T** (see E). This behavior corresponds to a large molecule and is a consequence of the introduction of two additional benzyl groups.

SPR competition tests showed no major alteration of the affinity of **7** for DC-SIGN relative to **2** and **3** (Table 1, DC-SIGN IC_{50} 254 μM). However, the cumulative modifications from **2** and **3** as assembled in **7** appeared to induce a drastic synergistic effect on selectivity against langerin. Indeed, no IC_{50} for **7** could be determined in the competition-langerin binding assay, since no inhibition was observed in the concentration range (up to 4.4 mM). Thus, no selectivity factor could be calculated. Gratifyingly, these data suggest that binding to langerin is excluded for **7**.

To further illuminate this finding, we evaluated the level of binding inhibition for both DC-SIGN and langerin using the maximal concentration sustainable in the assay (4.4 mM) with ligands from the natural ligand Manα1−2Man to the mimics **1**, **2**, **3**, and **7** (Table 1). At this high concentration, compounds **2** and **3** inhibit langerin 36.3% and 41.9%, respectively, while the DC-SIGN binding inhibition reaches almost 100% for both ligands. Remarkably, compound **7** results in almost 100% inhibition of DC-SIGN binding with no observed langerin inhibition.

Characterizations of Compound 7 Binding Properties to DC-SIGN. We further analyzed the interaction properties of **7** with DC-SIGN ECD by ITC. The pseudosaccharide **7** (4.7 mM) was titrated into lectin solution (566 μM). The ITC data of the titration of **7** to DC-SIGN ECD confirm the moderate affinity (Figure 6A). Fitting one binding site model to the data with an assumed stoichiometry value *n* fixed to 1 yielded a K_d of 171 ± 11 μM, which was in the same range as the apparent affinity determined by SPR competition assay (IC_{50} 254 μM). So far, the combination of the moderate affinity and a low molecular weight of these glycomimetics have precluded the evaluation of a K_d by SPR in a direct interaction mode. In addition, improvement of the affinity, below millimolar range, allows observation in real time of the glycomimetic binding on a DC-SIGN ECD functionalized surface. The resulting K_d is 310 μM for compound **7** (Figure 6B). From these different and complementary analyses, an affinity in the range of 250 μM can be assumed for **7**. The ITC analysis yielded a $\Delta H = -9.54 \pm 0.26$ kJ mol^{-1} and a $T\Delta S = 11.9$ kJ mol^{-1}, leading to a ΔG of −21.4 kJ mol^{-1}. Thus, the binding mode of **7** is almost equally enthalpically and entropically driven.

DISCUSSION AND CONCLUSIONS

CLRs are involved in numerous aspects of immune regulation, and they have attracted great interest as targets for anti-infective strategies, vaccine delivery, immune modulation, etc. However, due to their large open binding sites, their low affinity for their natural ligands, and the carbohydrate cross-recognition between some CLRs, the number of specific ligands is limited. Indeed, when considering only computed druggability scores, most CLRs were predicted to be challenging or even undruggable targets.[45] Despite this challenging task, recent progress has been made toward defining potent antagonists against CLRs, such as DC-SIGN, Mincle, and DCIR.[29,46,47] However, we are still far from compounds with the required affinity and the relevant specificity to envision their use in clinical trials.

To address specific difficulties encountered regarding selectivity, we defined, in this work, a new strategy to improve our rationally designed glycomimetics. DC-SIGN and langerin are CLRs for which development of a highly specific antagonist would be of great potential impact.[48] The rational design of compounds selective for DC-SIGN is very challenging due to its very open binding site, which is difficult to exploit (Figure 1C). Thus, instead of modifying the ligand by adding additional

DOI: 10.1021/acschembio.7b00958
ACS Chem. Biol. 2018, 13, 600−608

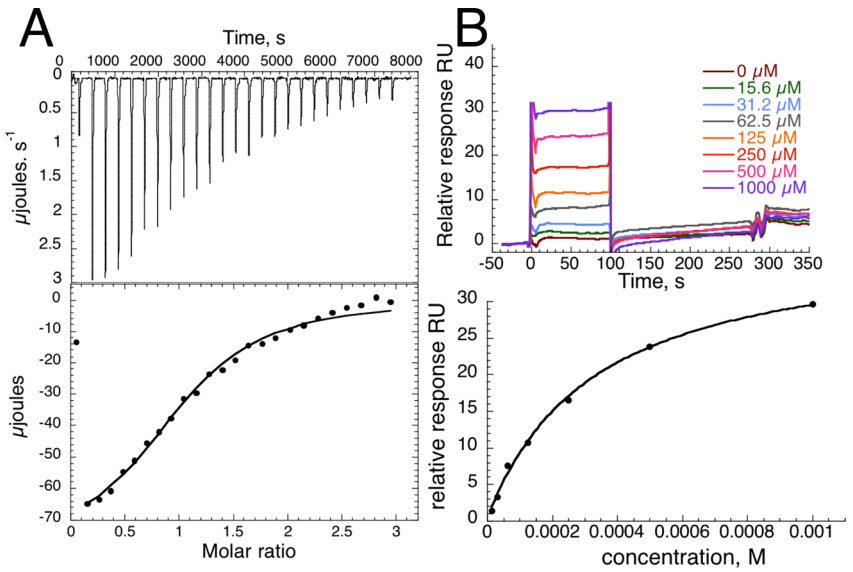

Figure 6. ITC and SPR analysis of glycomimetic **7** titration to DC-SIGN ECD. (A) Titration of glycomimetic **7** at 4.7 mM to DC-SIGN ECD (566 μM). Upper panel shows the titration thermogram and lower panel, the data integration with fitted curves (1:1 binding model). (B) Titration of glycomimetic **7** onto DC-SIGN ECD functionalized surface. Upper panel shows reference-subtracted sensorgrams of increasing concentrations of **7** and lower panel, the steady state binding analysis (1:1 binding model).

anchoring points within the targeted binding site, as in classical approaches, we searched for optimizations within our compounds that could impair their interaction within the langerin binding site. In order to do this, we first made a careful comparative analysis of the binding mode of natural ligands known to be specific for one of the two CLRs. Having defined the differential determinants between the CLR binding sites and their natural ligands, we can more completely understand the source of ligand selectivity. Indeed, we showed that residue K313 in the langerin binding site strongly interacts with a sulfate group at C_6 of the carbohydrate ligands. Then, we exploited this finding to introduce modifications that should selectively alter langerin recognition, while maintaining tight DC-SIGN binding. Exploiting the differences between both CLR binding sites and rational designed ligand modifications, this strategy succeeded in generating a highly specific compound for DC-SIGN. Following the evolution of **1** to **2** and **3** and finally to **7**, we have improved the selectivity with compound **7** to such a level that neither the interaction nor the selectivity factor with langerin are measurable. We can target DC-SIGN specificity rather than selectivity with the new compound developed in this work. Arguably, the structure of **7** and its DC-SIGN affinity may still be far from ideal for a potential drug. However, the strategy we used to develop it, where ligand improvements can be obtained through differential analysis between two competing receptors for a given ligand, can be of general use in the development of inhibitors. This approach is of particular interest when improvements in ligand/target affinity are limited by biophysical phenomena, as in the case of CLRs. Once the selectivity is achieved, the increase of affinity can be then reached by avidity effect through multivalent displaying of glycomimetics. In order to confirm the translation of the selectivity achieved with **7** into a real biological effect, such multivalent systems presenting **7** will have to be designed. Thus, future work will be centered on the synthesis of such avidity-improved systems and their evaluation in dedicated cellular infection assays.

MATERIALS AND METHODS

Compounds. The GlcNAc-sulfated derivatives (Figure 2A) were purchased from Dextra Laboratories.

DC-SIGN and Langerin ECD Production and Purification. WT and mutated recombinant forms of DC-SIGN and langerin extracellular domain (DC-SIGN ECD and Lg-ECD respectively) were produced and purified as described previously.[41,49]

Crystallization. Crystals of Lg-CRD were grown from a sample of Lg-ECD by the hanging-drop vapor-diffusion method at 293 K with a protein/reservoir drop ratio of 1:1, at a protein concentration of 15 mg mL^{-1} in 25 mM Tris-HCl at pH 8, 150 mM NaCl, and 4 mM $CaCl_2$ and a reservoir containing 100 mM HEPES at pH 7, 100 mM $MgCl_2$, 150 mM NaCl, and 20% PEG 3350 supplemented or not with 70 mM europium dipicolinate. The use of this lanthanide complex was motivated by the aim to crystallize the full-length langerin ECD protein by inducing interactions between the complex and arginine residues to promote crystal contacts.[50] Crystals appeared after 2 months with the typical Lg-CRD crystal shape and dimension described previously.[51] In drop proteolysis, by traces of proteases, of Lg-ECD between the CRD and the Neck domain of langerin account for this phenomenon. This was confirmed by evaluation of the space group and the cell dimension.

For Lg-CRD/GlcNS6S complex preparation, crystals were first washed in 100 mM HEPES at pH 7, 100 mM $MgCl_2$, 150 mM NaCl, and 35% PEG 3350 for cryoprotection and, second, soaked and equilibrated by vapor diffusion over 1 h in 1 μL of the previous solution supplemented with 10 mM GlcNS6S. Crystals were directly flash frozen in liquid nitrogen.

Data Collection, Processing, and Structure Determination. X-ray diffraction data were collected in the BM30a beamline at the ESRF Grenoble using an ADSC Q315r detector. The crystals was diffracted with a wavelength of 0.979 Å, exposition time of 20 s/images, 200 images with an angular step of 0.5°, and a detector distance of 220 mm. Data processing is described in the SI Structural Analysis section. Coordinates and associated structure factors have been deposited in the PDB database, code: 5g6u.

Surface Plasmon Resonance Analysis. Surface plasmon resonance experiments were performed on a Biacore 3000 using a CM4 chip, functionalized at 5 μL/min. Fc1 and Fc3 were prepared as reference surfaces. Flow cells (Fc) from 1 to 4 were activated with 50 μL of a 0.2 M EDC/0.05 M NHS mixture. After this step, Fc1 to Fc4 were respectively functionalized with bovine serum albumin (BSA)

DOI: 10.1021/acschembio.7b00958
ACS Chem. Biol. 2018, 13, 600−608

and mannosylated bovine serum albumin (BSA-Man, BSA-manα1−3[manα1−6]man, Dextra laboratories, 60 μg mL^{-1}). Then remaining activated groups of both cells were blocked with 30 μL of 1 M ethanolamine. After blocking, the four Fc's were treated with 5 μL of 10 mM HCl to remove unspecific bound protein and 5 μL of 50 mM EDTA to expose the surface to a regeneration protocol. Finally, 238 RU and 1847 RU of BSA and BSA-Man were respectively immobilized on Fc1 and Fc2.

For inhibition studies, on Fc2 or Fc4, 20 μM of DC-SIGN ECD or 15 μM of langerin ECD, respectively, are mixed with increasing concentrations of inhibiting compounds that were prepared in a running buffer composed of 25 mM Tris at pH 8, 150 mM NaCl, 4 mM $CaCl_2$, and 0.005% P20 surfactant, and 13 μL of each sample was injected onto the surfaces at a 5 μL/min flow rate. The resulting sensorgrams were reference surface corrected.

$$y = R_{hi} - \frac{R_{hi} - R_{lo}}{1 + \left(\frac{Conc}{A_1}\right)^{A_2}} \quad (1)$$

$$IC_{50} = A_1 \cdot \left(\left(\frac{R_{hi} - R_{lo}}{R_{hi} - 50} \right)^{1/A_2} - 1 \right) \quad (2)$$

The DC-SIGN binding responses were extracted from sensorgrams, converted to percent residual activity values (y), which were plotted against corresponding compound concentration. The four-parameter logistic model (eq 1), available in the BiaEval software, was fitted to the plots, and the IC_{50} values were calculated, from eq 2, using the values of fitted parameters (R_{hi}, R_{lo}, A_1, and A_2). The software is able to fit and to calculate an IC_{50} even if the 50% inhibition is not observed as it is in the case for one of the ligands in Figure 2.

Isothermal Titration Calorimetric analysis. ITC experiments were performed at 25 °C using a TA Instrument Nano Isothermal Titration Calorimeter Low Volume (Nano ITC LV) with a 190 μL cell volume. Compound **7** and DC-SIGN ECD were prepared in 25 mM Tris at pH 8, 150 mM NaCl, and 4 mM $CaCl_2$. The compound was stepwise injected (1.03 μL) into DC-SIGN solution using 5 min intervals between injections. Then, 566 μM of monomeric DC-SIGN ECD and 0.47 mM compound concentrations were used. The blank titrations (compounds to buffer) were done for subtraction of dilution heat from the integrated data. A one-site binding model was fit to the data (nanoAnalyse 2.20 TA), yielding association constants (K_A) and binding enthalpies (ΔH). The free energy changes (ΔG) and entropy (ΔS) were calculated using the following equation:

$$\Delta G = \Delta H - T\Delta S = -RT \ln K_A$$

where T is the absolute temperature and R = 8.314.

Synthesis. The 6-modified pseudodisaccharides **3**−**7** were synthesized starting from 6-azidomannose tetra-*O*-benzoate following procedures previously established for **1** and **2**. Full details are collected in the Supporting Information.

NMR Analysis. All NMR experiments were performed on a Bruker Avance DRX 500 MHz spectrometer equipped with a 5 mm inverse triple-resonance probe. All the samples were dissolved in 550 μL of buffer D_2O (150 mM NaCl, 4 mM $CaCl_2$, 25 mM d-Tris, pD 7.2) with a ligand concentration of 2 mM for free ligand analysis. For the experiments in the presence of receptor 19 or 9.5 μM of DC-SIGN and 1.0 mM of the ligand were used. The pD was adjusted to 7.2 in all samples. STD NMR experiments were carried out at 25 °C. For protein saturation, a train of Gaussian shaped pulses with a length of 49 ms, an interpulse delay of 1 ms, and an attenuation of 50 dB was used. The unwanted broad resonance signals of the protein were removed by use of a spin lock pulse of 15 ms prior to acquisition. For suppression of the water signal, the WATERGATE scheme (3−9−19) was employed. The on-resonance frequency was set to −1 ppm, whereas the off-resonance frequency was set to 40 ppm, interleaved recorded. Reference experiments were carried out to confirm the absence of direct irradiation of the ligand. Saturation times to obtain the build-up curves were 0.5, 1, 1.5, 2, 3, and 4 s. Additional experimental details are given in the Supporting Information.

■ ASSOCIATED CONTENT

Supporting Information

The Supporting Information is available free of charge on the ACS Publications website at DOI: 10.1021/acschembio.7b00958.

Structural analysis (Table S1, Figures S1 and S2), synthesis methods (Figures S3 and S4), compound characterizations (Figures S5, S6), SPR data for all competition studies with DC-SIGN and langerin (Figures S7−S9 and Table S2), and STD NMR data analysis (Figures S10−S12 and Tables S3 and S4) (PDF)

■ AUTHOR INFORMATION

Corresponding Authors

*E-mail: anna.bernardi@unimi.it.
*E-mail: franck.fieschi@ibs.fr.

ORCID

Anna Bernardi: 0000-0002-1258-2007
Franck Fieschi: 0000-0003-1194-8107

Notes

The authors declare no competing financial interest.

■ ACKNOWLEDGMENTS

This work used the platforms of the Grenoble Instruct center (ISBG; UMS 3518 CNRS-CEA-UGA-EMBL). SPR and MP3 platforms support from FRISBI (ANR-10-INSB-05-02) and GRAL (ANR-10-LABX-49-01) within the Grenoble Partnership for Structural Biology (PSB). This work was supported with funds from CM1102 COST Action and EU ITN Marie Curie program Immunoshape (Grant no. 642870). We are grateful to EU ITN Marie-Curie program (CARMUSYS − Grant no. 213592) for funding I.S. and N.V. V.P. was supported by la Région Rhône-Alpes. The authors thank C. Solera for NMR spectra acquisition and S. Temme for critical review of the manuscript.

■ REFERENCES

(1) van Vliet, S. J., García-Vallejo, J. J., and van Kooyk, Y. (2008) Dendritic cells and C-type lectin receptors: coupling innate to adaptive immune responses. *Immunol. Cell Biol. 86*, 580−587.

(2) Bell, D., Young, J. W., and Banchereau, J. (1999) Dendritic cells. *Adv. Immunol. 72*, 255−324.

(3) van Kooyk, Y., Engering, A., Lekkerkerker, A. N., Ludwig, I. S., and Geijtenbeek, T. B. (2004) Pathogens use carbohydrates to escape immunity induced by dendritic cells. *Curr. Opin. Immunol. 16*, 488−493.

(4) Geijtenbeek, T. B., van Vliet, S. J., Engering, A., t Hart, B. A., and van Kooyk, Y. (2004) Self- and nonself-recognition by C-type lectins on dendritic cells. *Annu. Rev. Immunol. 22*, 33−54.

(5) Powlesland, A. S., Fisch, T., Taylor, M. E., Smith, D. F., Tissot, B., Dell, A., Pöhlmann, S., and Drickamer, K. (2008) A novel mechanism for LSECtin binding to Ebola virus surface glycoprotein through truncated glycans. *J. Biol. Chem. 283*, 593−602.

(6) Zhao, D., Han, X., Zheng, X., Wang, H., Yang, Z., Liu, D., Han, K., Liu, J., Wang, X., Yang, W., Dong, Q., Yang, S., Xia, X., Tang, L., and He, F. (2016) The Myeloid LSECtin Is a DAP12-Coupled Receptor That Is Crucial for Inflammatory Response Induced by Ebola Virus Glycoprotein. *PLoS Pathog. 12*, e1005487.

(7) Geijtenbeek, T. B., Kwon, D. S., Torensma, R., van Vliet, S. J., van Duijnhoven, G. C., Middel, J., Cornelissen, I. L., Nottet, H. S., KewalRamani, V. N., Littman, D. R., Figdor, C. G., and van Kooyk, Y.

DOI: 10.1021/acschembio.7b00958
ACS Chem. Biol. 2018, 13, 600−608

(2000) DC-SIGN, a dendritic cell-specific HIV-1-binding protein that enhances trans-infection of T cells. *Cell 100*, 587−597.
(8) Geijtenbeek, T. B., van Vliet, S. J., Koppel, E. A., Sanchez-Hernandez, M., Vandenbroucke-Grauls, C. M., Appelmelk, B., and van Kooyk, Y. (2003) Mycobacteria target DC-SIGN to suppress dendritic cell function. *J. Exp. Med. 197*, 7−17.
(9) Cambi, A., Gijzen, K., de Vries, J. M., Torensma, R., Joosten, B., Adema, G. J., Netea, M. G., Kullberg, B. J., Romani, L., and Figdor, C. G. (2003) The C-type lectin DC-SIGN (CD209) is an antigen-uptake receptor for Candida albicans on dendritic cells. *Eur. J. Immunol. 33*, 532−538.
(10) Ernst, B., and Magnani, J. L. (2009) From carbohydrate leads to glycomimetic drugs. *Nat. Rev. Drug Discovery 8*, 661−677.
(11) Sattin, S., and Bernardi, A. (2016) Glycoconjugates and Glycomimetics as Microbial Anti-Adhesives. *Trends Biotechnol. 34*, 483−495.
(12) Anderluh, M., Jug, G., Svajger, U., and Obermajer, N. (2012) DC-SIGN antagonists, a potential new class of anti-infectives. *Curr. Med. Chem. 19*, 992−1007.
(13) Borrok, M. J., and Kiessling, L. L. (2007) Non-carbohydrate inhibitors of the lectin DC-SIGN. *J. Am. Chem. Soc. 129*, 12780−12785.
(14) Garber, K. C. A., Wangkanont, K., Carlson, E. E., and Kiessling, L. L. (2010) A general glycomimetic strategy yields non-carbohydrate inhibitors of DC-SIGN. *Chem. Commun. (Cambridge, U. K.) 46*, 6747−6749.
(15) Obermajer, N., Sattin, S., Colombo, C., Bruno, M., Svajger, U., Anderluh, M., and Bernardi, A. (2011) Design, synthesis and activity evaluation of mannose-based DC-SIGN antagonists. *Mol. Diversity 15*, 347−360.
(16) Andreini, M., Doknic, D., Sutkeviciute, I., Reina, J. J., Duan, J., Chabrol, E., Thépaut, M., Moroni, E., Doro, F., Belvisi, L., Weiser, J., Rojo, J., Fieschi, F., and Bernardi, A. (2011) Second generation of fucose-based DC-SIGN ligands: affinity improvement and specificity versus langerin. *Org. Biomol. Chem. 9*, 5778−5786.
(17) Becer, C. R., Gibson, M. I., Geng, J., Ilyas, R., Wallis, R., Mitchell, D. A., and Haddleton, D. M. (2010) High-affinity glycopolymer binding to human DC-SIGN and disruption of DC-SIGN interactions with HIV envelope glycoprotein. *J. Am. Chem. Soc. 132*, 15130−15132.
(18) Martínez-Avila, O., Hijazi, K., Marradi, M., Clavel, C., Campion, C., Kelly, C., and Penadés, S. (2009) Gold manno-glyconanoparticles: multivalent systems to block HIV-1 gp120 binding to the lectin DC-SIGN. *Chem. - Eur. J. 15*, 9874−9888.
(19) Sattin, S., Fieschi, F., and Bernardi, A. (2015) DC-SIGN as a Target for Drug Development Based on Carbohydrates. *Carbohydrate Chemistry: State of the Art and Challenges for Drug Development*, 379−394.
(20) Reina, J. J., Sattin, S., Invernizzi, D., Mari, S., Martinez-Prats, L., Tabarani, G., Fieschi, F., Delgado, R., Nieto, P. M., Rojo, J., and Bernardi, A. (2007) 1,2-Mannobioside mimic: synthesis, DC-SIGN interaction by NMR and docking, and antiviral activity. *ChemMedChem 2*, 1030−1036.
(21) Sattin, S., Daghetti, A., Thépaut, M., Berzi, A., Sánchez-Navarro, M., Tabarani, G., Rojo, J., Fieschi, F., Bernardi, A., and Clerici, M. (2010) Inhibition of DC-SIGN-mediated HIV infection by a linear trimannoside mimic in a tetravalent presentation. *ACS Chem. Biol. 5*, 301−312.
(22) Berzi, A., Reina, J. J., Ottria, R., Sutkeviciute, I., Antonazzo, P., Sánchez-Navarro, M., Chabrol, E., Cetin, I., Rojo, J., Fieschi, F., Bernardi, A., Clerici, M., Biasin, M., and Trabattoni, D. (2012) A glycomimetic compound inhibits DC-SIGN-mediated HIV infection in cellular and cervical explant models. *AIDS 26*, 127−137.
(23) Thépaut, M., Guzzi, C., Sutkeviciute, I., Sattin, S., Ribeiro-Viana, R., Varga, N., Chabrol, E., Rojo, J., Bernardi, A., Angulo, J., Nieto, P. M., and Fieschi, F. (2013) Structure of a Glycomimetic Ligand in the Carbohydrate Recognition Domain of C-type Lectin DC-SIGN. Structural Requirements for Selectivity and Ligand Design. *J. Am. Chem. Soc. 135*, 2518−2529.
(24) Sutkeviciute, I., Thépaut, M., Sattin, S., Berzi, A., McGeagh, J., Grudinin, S., Weiser, J., Le Roy, A., Reina, J. J., Rojo, J., Clerici, M., Bernardi, A., Ebel, C., and Fieschi, F. (2014) Unique DC-SIGN clustering activity of a small glycomimetic: A lesson for ligand design. *ACS Chem. Biol. 9*, 1377−1385.
(25) Guzzi, C., Alfarano, P., Sutkeviciute, I., Sattin, S., Ribeiro-Viana, R., Fieschi, F., Bernardi, A., Weiser, J., Rojo, J., Angulo, J., and Nieto, P. M. (2016) Detection and quantitative analysis of two independent binding modes of a small ligand responsible for DC-SIGN clustering. *Org. Biomol. Chem. 14*, 335−344.
(26) Varga, N., Sutkeviciute, I., Guzzi, C., McGeagh, J., Petit-Haertlein, I., Gugliotta, S., Weiser, J., Angulo, J., Fieschi, F., and Bernardi, A. (2013) Selective targeting of dendritic cell-specific intercellular adhesion molecule-3-grabbing nonintegrin (DC-SIGN) with mannose-based glycomimetics: synthesis and interaction studies of bis(benzylamide) derivatives of a pseudomannobioside. *Chem. - Eur. J. 19*, 4786−4797.
(27) Mitchell, D. A., Jones, N. A., Hunter, S. J., Cook, J., Jenkinson, S. F., Wormald, M. R., Dwek, R. A., and Fleet, G. W. J. (2007) Synthesis of 2-C-branched derivatives of D-mannose: 2-C-aminomethyl-D-mannose binds to the human C-type lectin DC-SIGN with affinity greater than an order of magnitude compared to that of D-mannose. *Tetrahedron: Asymmetry 18*, 1502−1510.
(28) Tomašić, T., Hajšek, D., Svajger, U., Luzar, J., Obermajer, N., Petit-Haertlein, I., Fieschi, F., and Anderluh, M. (2014) Monovalent mannose-based DC-SIGN antagonists: targeting the hydrophobic groove of the receptor. *Eur. J. Med. Chem. 75*, 308−326.
(29) Varga, N., Sutkeviciute, I., Ribeiro-Viana, R., Berzi, A., Ramdasi, R., Daghetti, A., Vettoretti, G., Amara, A., Clerici, M., Rojo, J., Fieschi, F., and Bernardi, A. (2014) A multivalent inhibitor of the DC-SIGN dependent uptake of HIV-1 and Dengue virus. *Biomaterials 35*, 4175−4184.
(30) Ordanini, S., Varga, N., Porkolab, V., Thépaut, M., Belvisi, L., Bertaglia, A., Palmioli, A., Berzi, A., Trabattoni, D., Clerici, M., Fieschi, F., and Bernardi, A. (2015) Designing nanomolar antagonists of DC-SIGN-mediated HIV infection: ligand presentation using molecular rods. *Chem. Commun. (Cambridge, U. K.) 51*, 3816−3819.
(31) Bernardi, A., Jiménez-Barbero, J., Casnati, A., De Castro, C., Darbre, T., Fieschi, F., Finne, J., Funken, H., Jaeger, K.-E., Lahmann, M., Lindhorst, T. K., Marradi, M., Messner, P., Molinaro, A., Murphy, P. V., Nativi, C., Oscarson, S., Penadés, S., Peri, F., Pieters, R. J., Renaudet, O., Reymond, J.-L., Richichi, B., Rojo, J., Sansone, F., Schäffer, C., Turnbull, W. B., Velasco-Torrijos, T., Vidal, S., Vincent, S., Wennekes, T., Zuilhof, H., and Imberty, A. (2013) Multivalent glycoconjugates as anti-pathogenic agents. *Chem. Soc. Rev. 42*, 4709−4727.
(32) Cecioni, S., Imberty, A., and Vidal, S. (2015) Glycomimetics versus multivalent glycoconjugates for the design of high affinity lectin ligands. *Chem. Rev. 115*, 525−561.
(33) de Witte, L., Nabatov, A., Pion, M., Fluitsma, D., de Jong, M. A. W. P., de Gruijl, T., Piguet, V., van Kooyk, Y., and Geijtenbeek, T. B. H. (2007) langerin is a natural barrier to HIV-1 transmission by Langerhans cells. *Nat. Med. 13*, 367−371.
(34) de Witte, L., Nabatov, A., and Geijtenbeek, T. B. H. (2008) Distinct roles for DC-SIGN+-dendritic cells and Langerhans cells in HIV-1 transmission. *Trends Mol. Med. 14*, 12−19.
(35) de Jong, M. A. W. P., and Geijtenbeek, T. B. H. (2010) Langerhans cells in innate defense against pathogens. *Trends Immunol. 31*, 452−459.
(36) van den Berg, L. M., Ribeiro, C. M. S., Zijlstra-Willems, E. M., de Witte, L., Fluitsma, D., Tigchelaar, W., Everts, V., and Geijtenbeek, T. B. H. (2014) Caveolin-1 mediated uptake via langerin restricts HIV-1 infection in human Langerhans cells. *Retrovirology 11*, 3903.
(37) Galustian, C., Park, C. G., Chai, W., Kiso, M., Bruening, S. A., Kang, Y.-S., Steinman, R. M., and Feizi, T. (2004) High and low affinity carbohydrate ligands revealed for murine SIGN-R1 by carbohydrate array and cell binding approaches, and differing specificities for SIGN-R3 and langerin. *Int. Immunol. 16*, 853−866.

DOI: 10.1021/acschembio.7b00958
ACS Chem. Biol. 2018, 13, 600−608

(38) Feinberg, H., Taylor, M. E., Razi, N., Mcbride, R., Knirel, Y. A., Graham, S. A., Drickamer, K., and Weis, W. I. (2011) Structural basis for langerin recognition of diverse pathogen and mammalian glycans through a single binding site. *J. Mol. Biol. 405*, 1027−1039.
(39) Chabrol, E., Nurisso, A., Daina, A., Vassal-Stermann, E., Thépaut, M., Girard, E., Vivès, R. R., and Fieschi, F. (2012) Glycosaminoglycans are interactants of langerin: comparison with gp120 highlights an unexpected calcium-independent binding mode. *PLoS One 7*, e50722.
(40) Muñoz-García, J. C., Chabrol, E., Vivès, R. R., Thomas, A., de Paz, J. L., Rojo, J., Imberty, A., Fieschi, F., Nieto, P. M., and Angulo, J. (2015) langerin-heparin interaction: two binding sites for small and large ligands as revealed by a combination of NMR spectroscopy and cross-linking mapping experiments. *J. Am. Chem. Soc. 137*, 4100−4110.
(41) Thépaut, M., Valladeau, J., Nurisso, A., Kahn, R., Arnou, B., Vivès, C., Saeland, S., Ebel, C., Monnier, C., Dezutter-Dambuyant, C., Imberty, A., and Fieschi, F. (2009) Structural studies of langerin and Birbeck granule: a macromolecular organization model. *Biochemistry 48*, 2684−2698.
(42) Tateno, H., Ohnishi, K., Yabe, R., Hayatsu, N., Sato, T., Takeya, M., Narimatsu, H., and Hirabayashi, J. (2010) Dual Specificity of langerin to Sulfated and Mannosylated Glycans via a Single C-type Carbohydrate Recognition Domain. *J. Biol. Chem. 285*, 6390−6400.
(43) Feinberg, H., Rowntree, T. J. W., Tan, S. L. W., Drickamer, K., Weis, W. I., and Taylor, M. E. (2013) Common polymorphisms in human langerin change specificity for glycan ligands. *J. Biol. Chem. 288*, 36762−36771.
(44) Angulo, J., Ardá, A., Cabrita, E. J., Martin-Pastor, M., Jiménez-Barbero, J., and Nieto, P. M. (2015) NMR Techniques for the Study of Transient Intermolecular Interactions, in Structure Elucidation in Organic Chemistry (Bravo, M. M., Ed.), pp 325−360, Wiley-VCH, Weinheim, Germany.
(45) Aretz, J., Wamhoff, E.-C., Hanske, J., Heymann, D., and Rademacher, C. (2014) Computational and experimental prediction of human C-type lectin receptor druggability. *Front. Immunol. 5*, 323.
(46) Feinberg, H., Jégouzo, S. A. F., Rowntree, T. J. W., Guan, Y., Brash, M. A., Taylor, M. E., Weis, W. I., and Drickamer, K. (2013) Mechanism for recognition of an unusual mycobacterial glycolipid by the macrophage receptor mincle. *J. Biol. Chem. 288*, 28457−28465.
(47) Lambert, A. A., Azzi, A., Lin, S.-X., Allaire, G., St-Gelais, K. P., Tremblay, M. J., and Gilbert, C. (2013) Dendritic cell immunoreceptor is a new target for anti-AIDS drug development: identification of DCIR/HIV-1 inhibitors. *PLoS One 8*, e67873.
(48) Wamhoff, E.-C., Hanske, J., Schnirch, L., Aretz, J., Grube, M., Varón Silva, D., and Rademacher, C. (2016) (19)F NMR-Guided Design of Glycomimetic langerin Ligands. *ACS Chem. Biol. 11*, 2407−2413.
(49) Tabarani, G., Thépaut, M., Stroebel, D., Ebel, C., Vivès, C., Vachette, P., Durand, D., and Fieschi, F. (2009) DC-SIGN neck domain is a pH-sensor controlling oligomerization: SAXS and hydrodynamic studies of extracellular domain. *J. Biol. Chem. 284*, 21229−21240.
(50) Pompidor, G., D'Aléo, A., Vicat, J., Toupet, L., Giraud, N., Kahn, R., and Maury, O. (2008) Protein Crystallography through Supramolecular Interactions between a Lanthanide Complex and Arginine. *Angew. Chem., Int. Ed. 47*, 3388−3391.
(51) Thépaut, M., Vivès, C., Pompidor, G., Kahn, R., and Fieschi, F. (2008) Overproduction, purification and preliminary crystallographic analysis of the carbohydrate-recognition domain of human langerin. *Acta Crystallogr., Sect. F: Struct. Biol. Cryst. Commun. 64*, 115−118.

DOI: 10.1021/acschembio.7b00958
ACS Chem. Biol. 2018, 13, 600−608